J Mater Sci (2007) 42:9075–9082
DOI 10.1007/s10853-007-1894-1

Laser-induced anisotropy in Ag^+-doped glasses

Arashmid Nahal · Fariba Moslehirad

Received: 22 January 2007 / Accepted: 29 May 2007 / Published online: 27 July 2007

Abstract An induced optical anisotropy is observed as a result of interaction of a high-power CW Ar^+ laser beam, with silver-ion-exchanged glasses. We have shown that the absorption of the beam by the thin layer of Ag^+ produces a temperature gradient resulting in a radial stress on the surface of the sample. The induced anisotropy makes the sample behave as a thin uniaxial optical medium with axis along the direction of the beam propagation. For the polarized light, the induced anisotropy restricts the application of micro-lenses, which are made by this method. The average refraction index of the interaction area is measured.

Introduction

It is well-known that placing an anisotropic absorbing crystal between two crossed polarizers and illuminating it with a white light, results in the appearance of a characteristic image with isogyres and isochromates, called the conoscopic pattern [1].

Induced anisotropy as a thermal effect of the interaction of light (laser beam, flash lamp,...) with crystals and some other amorphous materials, leading to formation of conoscopic patterns, has already been observed and studied by many researchers [2–14]. In all above-mentioned cases, especially the laser materials, the light induced anisotropy causes the interacted medium to behave as an optically uniaxial one, with the optical axis along the direction of the beam propagation. It is possible to induce similar effects by unpolarized light [15]. Interaction of Ag-containing thin layers with polarized laser beam could make the material anisotropic, leading to a dichroism [16–18], which is out of the scope of the present article.

In laser materials such as Nd^+: YAG rod, the temperature gradient created by the flash lamp generates a mechanical stress in the material, which leads to a thermal strain resulting in the appearance of a birefringence [6–8, 14]. Irradiating crystals such as $Tb_3Ga_5O_{12}$ or semiconductor-doped glasses by a laser beam also results in generation of stress birefringence (Δn) [4, 5, 10, 12, 13, 19], due to the thermal gradient induced by the Gaussian laser beam. In above-mentioned cases if one places the interacting medium between two crossed polarizers and illuminate it with a white light, a characteristic conoscopic pattern could be observed. This pattern means that a distinguished direction is induced (z-direction, along the propagation of the laser beam), which coincides with the dielectric principal axis ε_z i.e. $\varepsilon_x = \varepsilon_y \neq \varepsilon_z$. Thus, the medium becomes optically uniaxial similar to the case of a natural crystal [1]. The magnitude of Δn increases with the radius, by quadratic law [5]. Therefore, a linearly polarized light passing through the sample will experience a phase difference between the two components along n_r and n_ϕ (the radial and tangential photoelastic changes in the index of refraction, respectively). Thus, except for points located along the directions of the polarizer and the analyzer (x and y) for which the polarization remains linear, at each point of the transverse section, a polarization change yields a spatial elliptical polarization pattern.

We have observed the same phenomenon during the interaction of a CW Ar^+ laser beam (P_{max} = 8 W), working

A. Nahal (✉)
Department of Physics, University of Tehran, Karegar Shomali Ave., Tehran 14399-55961, Iran
e-mail: nahal@khayam.ut.ac.ir

F. Moslehirad
Qazvin Branch, Azad University, Daneshgah Ave., P.O. Box 34185-1416, Qazvin, Iran

in the multiline regime with Ag^+-doped glasses. Absorption of the laser beam energy by the thin layer of the embedded silver ions in the glass matrix increases the temperature of the incident point of the laser beam on the sample. The Gaussian intensity distribution of the beam results in establishing a temperature gradient across the incident point leading to the appearance of a stress birefringence in the sample. We have found that if one put the irradiated sample between two crossed polarizers, using white light, then a characteristic conoscopic pattern would be observed. That is, the irradiated ion-exchanged glass behaves as uniaxial optical medium, with axis along the beam propagation. This effect has not been studied for silver-ion-exchanged glasses neither reported for thin layer of silver ions in a glass matrix.

Doping a glass matrix with metal clusters produces a nonlinear optical medium, which is promising for opto-electronics applications like optical switches and slab waveguides. One of the most investigated doped glasses is the Na^+–Ag^+ ion-exchanged one. Studying the interaction of a high-power laser beam with Ag^+-doped glass develops our knowledge about the limits of the above-mentioned optical material, and also the temporary and permanent physical changes, which happen during and after the interaction. Here we report one of the effects (the induced optical anisotropy), which we have observed. There are other effects, as the results of the interaction of a high-power laser beam with Ag^+-doped glass, which we have reported elsewhere in detail [17, 20, 21].

Our experimental results show clearly that the micro-lenses produced by irradiating the ion-exchanged glass using a high-power laser beam [22, 23] are not suitable for use with polarized white light, due to the induced optical anisotropy in it. This important point should be considered during the production of above-mentioned micro-lenses. Local heating of doped glasses or polymers by a laser beam could produce a micro-lense. The formation of the micro-lens occurs, due to the local melting of subsurface layer of the glass. The glass melting causes by an increase of the light absorption with temperature. Thus, when laser radiation heats the glass the light penetration depth decreases, and in spite of the thermal diffusion the process of heat deposition becomes increasingly localized at the surface of the glass. This thermal runaway causes the host glass to melt locally under laser radiation. Because of the lower density of the molten glass compared with that of the solid glass, the material wells out and solidifies forming a micro-lense [22, 23]. Micro-lenses have many applications such as microlense array for telescope application [24], micro-lense-based projection displays [25] and etc.

The organization of the paper is as follows. In Sect. "Experiment", the experimental setup would be explained in detail the results of the experiments are reported in this section. The Sect. "Discussion" includes a preliminary explanation of the obtained results. The conclusion of report is given in the last section.

Experiment

Sample preparation

The samples are prepared using the well-known ion-exchange method [26]. For this, slides of commercial soda-lime glasses ($20 \times 30 \times 0.8$ mm) were placed in mixed molten salts of $NaNO_3/AgNO_3$ (96/4 wt.%) in a temperature of 400 °C for 4 h, in the atmospheric pressure. In the ion-exchange process some of the sodium ions of the glass matrix would be exchanged by some of the silver ions of the molten mixed salt, due to the diffusion process. The temperature and duration time of the ion-exchange process determines the concentration, diffusion depth in the matrix, and even the size of the formed silver ionic clusters in the glass matrix. The composition of the glass also affects the above-mentioned parameters. As a result, a thin layer of ion-exchanged glass would be formed in the glass substrate. In our experiments the average thickness of the ion-exchanged layer was about 180 μm, measured by a microscope equipped with a micrometer. Then the prepared samples were irradiated by a CW high-power Ar^+ laser beam (P_{max} = 8 W), working in multiline regime.

The ion-exchanged glass has a brownish color with a continuous absorption spectra in visible region with a peak in the UV region at about wavelength λ_a = 310 nm (Fig. 1), which is related to very small ionic silver clusters [27, 28]. The color of the incident point of the laser on the sample becomes yellowish after the interaction, with an orange colored periphery, which is made out of silver neutral clusters.

Interaction with the laser beam

The setup shown in Fig. 2 was used for studying the thermal effect of the laser beam on the optical properties of the ion-exchanged glass in real time.

The sample was placed in front of the Ar^+ laser with a little tilt to prevent back-reflection of the beam from the sample towards the laser cavity. An expanded linearly polarized He–Ne laser beam and a polaroid plate, placed after the sample, were used as a probe (P_{probe} = 1 mW) to study the induced-optical anisotropy and any optical path changes during the interaction, in real time. The transmitted probe beam was used to study the induced anisotropy, and the reflected beams from both sides of the sample were used to study the optical path changes (Fig.2).

Our experiments show that by increasing the power of the Ar^+ laser beam, the temperature of the incident point of

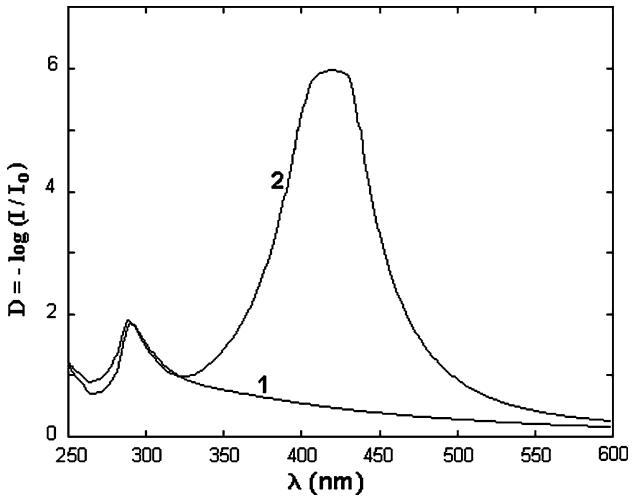

Fig. 1 The absorption spectra of an ion-exchanged glass: (1) before the interaction; (2) after the interaction. The peak around the wavelength 310 nm is related to existence of very small ionic silver clusters. The peak around the wavelength 430 nm is related to the surface palsmon resonance of the produced neutral silver clusters

the beam on the sample rises. Greater than a power threshold ($P_{th} \approx 4$ W, for ion-exchanged samples at 400 °C for 4 h) a conoscopic pattern appears on the screen behind the polaroid for the transmitted polarized probe beam (Fig. 2, down-left), and at the same time the interference pattern of the reflected probe beam becomes twisted at the place of the incident point (Fig. 2, down-right). Simultaneously, the reflected argon laser beam expands rapidly and at the end of the interaction forms co-centered rings on the screen behind the laser (Fig. 2, top-left). The same co-centered rings have been observed by other researchers during the interaction of laser beams with photorefractive crystals [29] and liquid crystals [30], as a thermal effect of the interaction. This pattern means that a thermal lens is formed. All the real-time observations of this experiment (conoscopic pattern, twisted interference pattern, and the co-centered rings pattern) indicate that, as a result of the thermal effect due to the interaction of the CW Ar^+-laser beam with the thin layer of the silver-ion-exchanged glass, a thermal lens and an optical anisotropy are induced into the sample.

The same conoscopic patterns, as those obtained in the real-time study, are observed when we put the sample (after the interaction) between two crossed polarizers which are illuminated with a white light (Figs. 3, 4a). The conoscopic pattern is also observed, for the case, when the polarizer and analyzer are parallel, but the dark and bright parts are complementary relative to the case when the polarizers were crossed (Fig. 4b). As it can be seen from the Fig. 4b, the isochromates for the blue light is placed closer to the center, relative to the isochromates for the red light. An orange circle also is seen (Fig. 4b), which is related to the silver nanoparticles on the surface of the sample [17, 20]. The produced micro-lens can be seen in Fig. 4b. From Fig. 4a, also it can be seen that, when the polarizer and the analyzer are crossed the first and third quadrants of the conoscopic pattern have a dominant blue color and the second and forth quadrants of the conoscopic pattern have a dominant yellow color. According to the Refs. [1, 31] the above-mentioned blue and yellow quadrants in the characteristic pattern are observed for optically positive uniaxial medium. Because of the remained thermal stress, the produced micro-lenses by this method are very unstable mechanically and would be cracked even with very little pressure on the sample. Thus, one should be careful with the samples after the interaction.

Measurement of average index of refraction of the interaction area

It would be useful if we could have some idea about the index of refraction of the interaction area. As the glass matrix melts during the interaction, and at the same time the silver ions reduce to the neutral ones, and also simultaneously the produced silver nanoparticles move toward the periphery, so that the index of refraction of the interaction area changes. On the other hand, the thermal effect of the beam changes the surface of the sample and produces a lens-like surface profile. Therefore, twisting of the fringes of the interference pattern, shown in down-right of Fig. 2, includes information about both the index changes and also modification of the profile of the surface. In order to measure the average index of refraction of the interaction area we use Fig. 2 (down-right). A schematic draw is shown in Fig. 5 to explain how the average index of refraction is measured. From Figs. 2, 5 and knowing the condition for constructive interference for the lights (He–Ne laser: probe) which have reflected from both side of the sample [32] we can write:

$$2n_i x = \lambda_1 \quad \text{(constructive interference)} \tag{1}$$

where x is the thickness equivalent to a difference of height for neighboring fringes, $\lambda_1 = 632.8$ nm is the wavelength of the probe laser beam and n_i is the index of refraction of the sample within the interacted area. From Fig. 5 if we take the average slope of the surface of the interacted area equal to β, and the inter-fringes for neighboring fringes as Δl, then we can write:

$$\tan\beta = \frac{x}{\Delta l} \tag{2}$$

for the small angle: $\tan\beta \approx \beta$, then from Eqs. 1 and 2 we have:

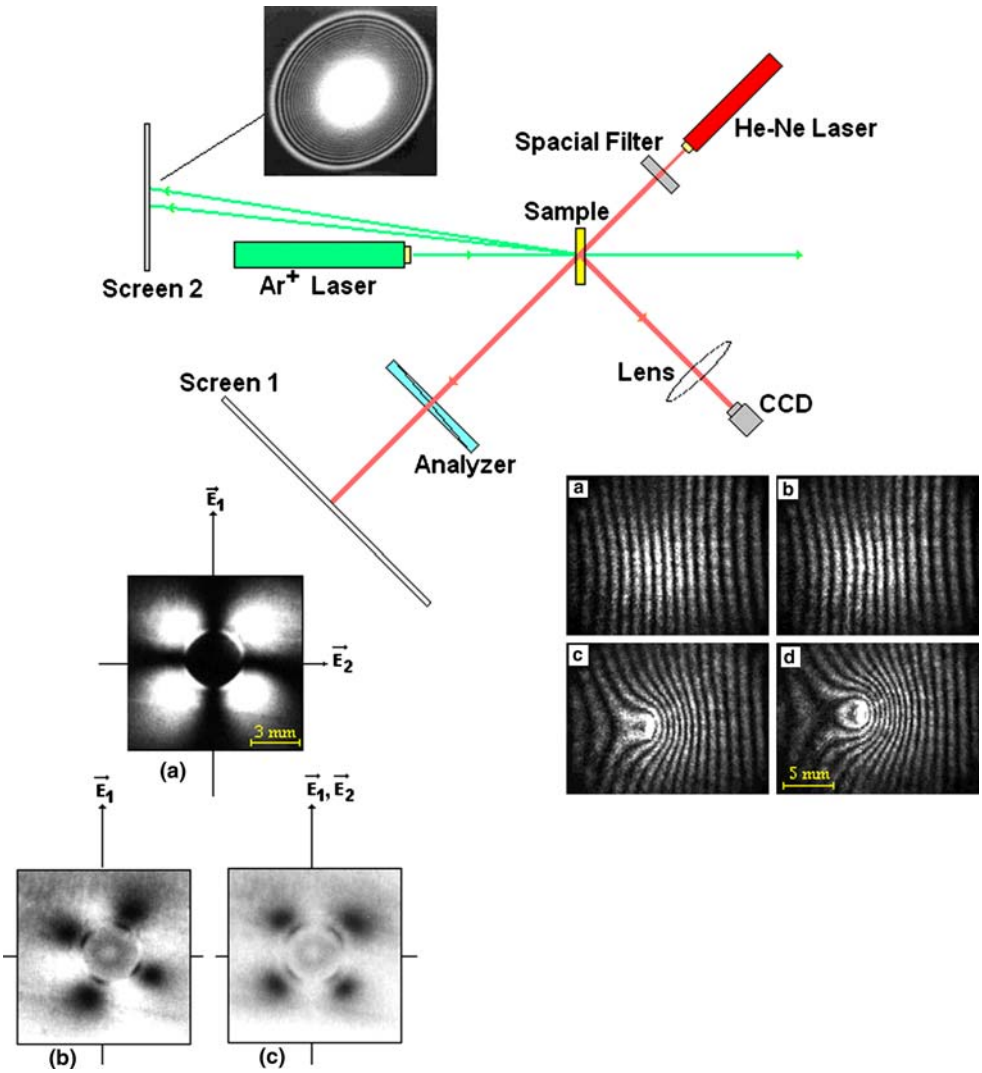

Fig. 2 The real-time study setup. After the interaction the reflection of the Argon laser beam from the interaction area forms the co-centered circular interference fringes (top-left). The conoscopic pattern appears on the screen for the transmitted probe beam (down-left), and for the reflected probe beam the fringes of the interference pattern would be twisted after the interaction (down-right). The conoscopic patterns are shown for three cases when (**a**) $\vec{P}\perp\vec{A}$; (**b**) $\angle(\vec{P},\vec{A}) = 45°$; and (**c**) $\vec{P}||\vec{A}$, respectively

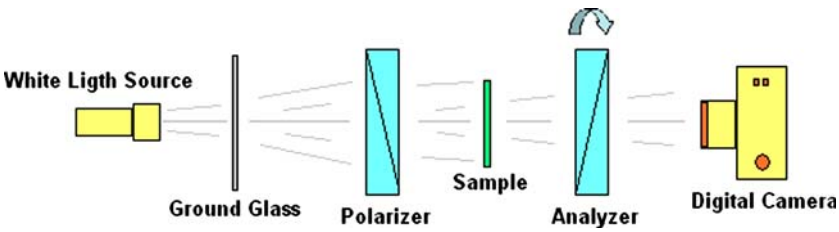

Fig. 3 The setup for studying the conoscopic patterns of the irradiated sample with white light

$$\beta = \frac{\lambda_1}{2n_i\Delta l} \tag{3}$$

Now if we rewrite the relation of Eq. 3 for p fringes, which occupy length l on the sample, we obtain:

$$\beta = \frac{p\lambda_1}{2n_i l} \tag{4}$$

On the other hand we can measure the height of the produced microlens, using the interferometric methods. In order to do this, we placed the curved surface of the sample on a test plate (roughness: $\lambda/20$), and illuminated it with a standard sodium lamp (λ_2 = 589.3 nm). The same twisted interference pattern, as in Fig. 2, would be formed, but this time for the air layer between the sample and the test plate. In this case we have the same relation as Eq. 4, but with q fringes in the length l for the wavelength λ_2, and n_{air} = 1:

$$\beta = \frac{q\lambda_2}{2l} \tag{5}$$

Then from Eqs. 4 and 5, the average index of refraction of the interaction is given by:

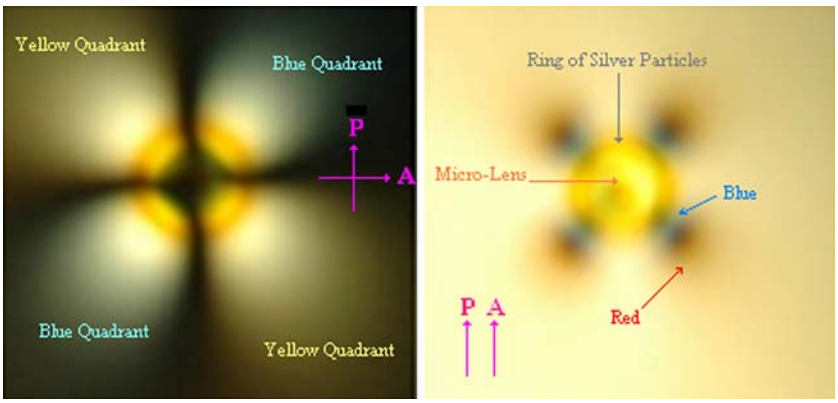

Fig. 4 The conoscopic patterns of the irradiated sample, using the setup shown in Fig. 3. (**a**) The conoscopic pattern for the case when $\vec{P} \perp \vec{A}$, and (**b**) for the case when $\vec{P} || \vec{A}$. It is seen that the isochromates for the blue color have smaller radius in comparison with the red one

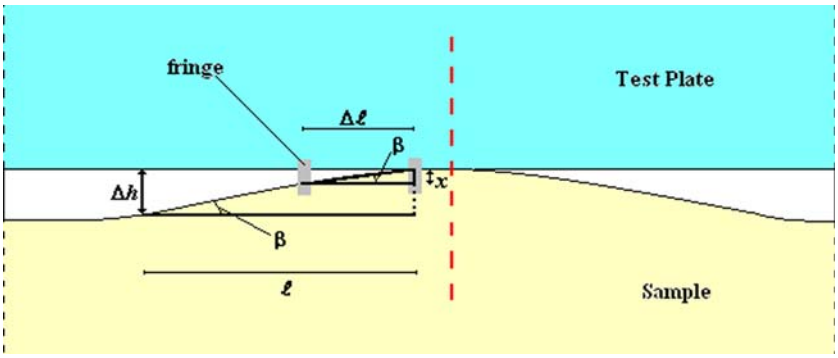

Fig. 5 A schematic drawing for showing the parameters, used to measure the average index of refraction of the interacted area on the sample. β is the slope of the modified surface, Δl is the distance between two neighboring fringes, l is the distance occupied by p number of fringes, Δh is the height of the produced thermal lens, and x is the height difference between two neighboring fringes

$$n_i = \frac{p\lambda_1}{q\lambda_2} \tag{6}$$

In our measurements we obtained $p = 13$, $q = 9$, with $\lambda_1 = 632.8$ nm, and $\lambda_2 = 589.3$ nm, respectively. Then relation of Eq. 6 gives: $n_i = 1.551$. Using the Brewster's angle measurement for He–Ne laser beam for $\lambda = 632.8$ nm the index of refraction of the non-interacted area on the sample is: $n_n = 1.549$. Thus, $\delta n = n_i - n_n \approx 0.002$. Our experimental results show that the average index of refraction of the interaction area has a little increase in its value relative to those parts which are not irradiated. This increase should be related to the reduction of silver ions to the neutral ones, and also to the concentration of silver nanoparticles near the periphery of the interaction area (orange ring in Fig. 4b) [20].

Using the interfrometric method the height of the generated thermal lens on the sample (4% $AgNO_3$, 400 °C, 4 h) was measured equal to $\Delta h \approx 6$ μm for $P_{max} = 8$ W.

Discussion

In this section we give a preliminary explanation for our experimental observations, which are reported in this article.

As shown in Fig. 1, the Ag^+-doped glass has an absorption in whole visible spectrum, with a peak in wavelength $\lambda_a = 310$ nm, leading to the brownish color for the ion-exchanged glass. This spectrum allows the sample to absorb the Ar^+ laser radiation, which results in heating the sample, locally, at the incident point of the laser beam and generation of neutral silver nanoparticles, with an absorption band peak about $\lambda_b = 410$ nm [17], resulting in the yellowish color of the interaction area. At the same time, because of the increase in the temperature, the interaction area melts and a micro-lens forms. Simultaneously, the produced silver nanoparticles move toward the periphery of the interaction area [17, 20, 22, 23]. The pushed silver nanoparticles make an orange colored ring on the sample (Fig. 4b). The melting of the glass matrix at the incident point of the laser generates a radial thermal gradient from center toward the periphery of the interaction area, which results in inducing a stress birefringence. Hence, in the interaction area both the index of refraction and the thickness of the medium will be changed. The whole thermal effect makes the irradiated sample act as a thin uniaxial anisotropic optical medium, with optical axis along the direction of beam propagation. Therefore, placing the interacted sample between two crossed polarizers results in appearance of the conoscopic pattern.

Let us have a brief review for propagation of light in an optical anisotropic medium, which results in forming the conoscopic patterns. When a light beam under an incident angle θ_1 enters into an anisotropic medium with thickness d, the beam is broken up into two beams with different refractive indices n', n'', where $\lambda' = \frac{\lambda}{n'}$, $\lambda'' = \frac{\lambda}{n''}$; with λ the wavelength in the vacuum. Hence, they propagate in the medium with different velocities, which results in retardation between them. That is, the exiting beams from the medium according to the Fig. 6a, have a phase difference equal to (see the Appendix A):

$$\delta = \frac{2\pi d}{\lambda}\left(\frac{n_o}{n_e}\sqrt{n_e^2 - \sin^2\theta_1} - n_o\sqrt{1 - \left(\frac{\sin\theta_1}{n_o}\right)^2}\right) \tag{7}$$

where n_o and n_e are the ordinary and extraordinary indices of refraction, respectively.

Leaving the medium, the two light beams with the phase difference λ = 632.8 nm could interfere. Now, if one places the anisotropic medium between a crossed polarizer and an analyzer ($\vec{P}$ and $\vec{A}$, respectively), with general angle χ between them, the characteristic intensity distribution could be observed. Let us take $\vec{D}_o$ for vibration direction of the ordinary beam and $\vec{D}_e$ for vibration direction of the extraordinary beam, with $\vec{D}_e \perp \vec{D}_o$ (Fig. 6b). Taking $\overrightarrow{OE}$ for amplitude of the incident beam, from Fig. 6b:

$$\begin{aligned}\overrightarrow{OB} &= \overrightarrow{OE}\cos\phi \\ \overrightarrow{OC} &= \overrightarrow{OE}\sin\phi\end{aligned} \tag{8}$$

where ϕ is the angle between $\vec{P}$ and $\vec{D}_o$. The analyzer just passes those components that are parallel to $\overrightarrow{OA}$:

$$\begin{aligned}\overrightarrow{OF} &= \overrightarrow{OB}\cos(\phi - \chi) \\ \overrightarrow{OG} &= \overrightarrow{OC}\sin(\phi - \chi)\end{aligned} \tag{9}$$

The two output beams could interfere, resulting in the intensity distribution:

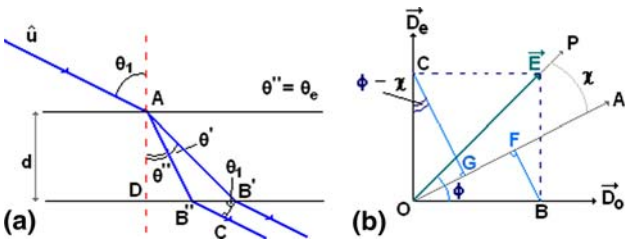

Fig. 6 (**a**) Refraction of a light beam entering into a birefringent medium. θ_1 is the incident angle, d is the thickness of the medium. (**b**) The diagram used to calculate the intensity distribution for the sample placed between the polarizer and the analyzer. χ is the angle between the polarizer and the analyzer, ϕ is the angle between the polarizer and the direction of $\mathbf{D}_o$

$$I = I_1 + I_2 + 2\sqrt{I_1 I_2}\cos\delta \tag{10}$$

where $I_1 = \left|\overrightarrow{OF}\right|^2$, $I_2 = \left|\overrightarrow{OG}\right|^2$. Using Eqs. 8, 9, and 10 the intensity distribution right after the analyzer would be equal to:

$$\frac{I}{I_\circ} = \cos^2\chi - \sin 2\phi \sin 2(\phi - \chi)\sin^2\frac{\delta}{2} \tag{11}$$

where $I_\circ = \left|\overrightarrow{OE}\right|^2$.

For the case when $\vec{P} \perp \vec{A}$ ($\chi = \frac{\pi}{2}$) we have:

$$\frac{I}{I_\circ} = \sin^2 2\phi \sin^2\frac{\delta}{2} \tag{12}$$

and for the case when $\vec{P} \| \vec{A}$ (χ = 0) we have:

$$\frac{I}{I_\circ} = 1 - \sin^2 2\phi \sin^2\frac{\delta}{2} \tag{13}$$

It is clear that, in the two above-mentioned cases the patterns are complementary to each other. Thus, the relation of Eq. 11 gives the intensity distribution of the conoscopic patterns for the case when the anisotropic optical medium is placed between the polarizer and the analyzer. In the Ref. [4], authors give a relation from which, using the parameters of the conoscopic pattern and the sample, one can estimate the induced birefringence Δn:

$$\Delta n = \frac{N\lambda}{L_{\text{eff}}} \tag{14}$$

where, λ is the wavelength of the light, N is the number of the fringes in the conoscopic pattern and L_{eff} is the thickness of the anisotropic medium. In our case: L_{eff} = 180 μm, λ = 550 nm (average wavelength for the white light) and N = 1 (Fig. 4). Thus, from Eq. 14 we obtain Δn = 0.003. It should be mentioned that the diffusion of silver ions into the glass substrate produces a thin layer, for which the concentration of silver ions and consequently the refractive index follow, in general, an exponential dependence [33, 34]. Thus, it is not easy to specify a sharp boundary between the doped layer and the substrate. Because of that, an effective thickness is introduced.

On the basis of the relations between Eqs. 12 and 13, using parameters of our samples we calculated the conoscopic patterns for both cases when $\vec{P} \perp \vec{A}$ and $\vec{P} \| \vec{A}$. The results are shown in Fig. 7. It can be seen that the experimental results (Fig. 4) and the calculation (Fig. 7) are consistent.

From Eq. 11 one can see that there is a dependence of intensity distribution of the conoscopic pattern on the wavelength of the light. We have drawn the interference

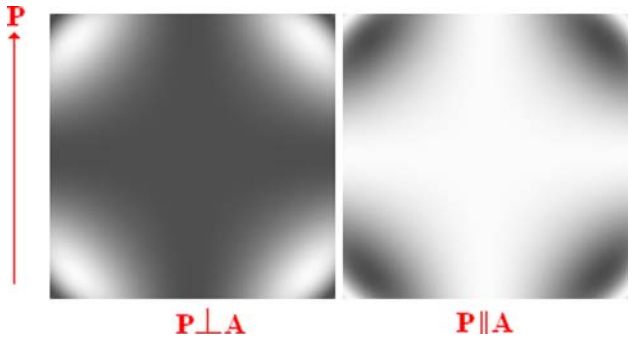

Fig. 7 The simulated conoscopic patterns for an irradiated sample, for two cases when the polarizer and the analyzer were perpendicular and parallel to each other, respectively. For the calculations the experimental results, measured in our samples, were used

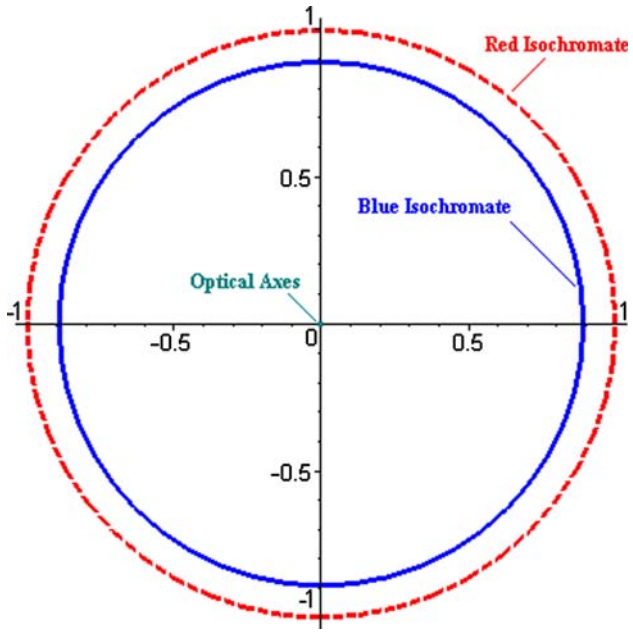

Fig. 8 The calculated isochromates for our samples using the relation of Eq. 11. The blue isochromate (bold circle) has smaller radius in comparison to the red one (the dashed circle). Their values are normalized to one, for simplicity. This calculation is in good accordance to the experimental results (Fig. 4b)

isochromates for both blue and red lights (Fig. 8) using the parameters of our samples. It can be seen that the isochromates of blue light have smaller radius relative to the isochromates of red light for the same order of interference. Our experimental results (Fig. 4b) show the same result for the irradiated Ag^+-doped glass by the Ar^+ laser beam. As it can be seen from Fig. 4b the blue fringes are closer to the center compared to the red ones.

Conclusion

In this article, we have reported the observation of an induced optical anisotropy in Ag^+-doped glasses as a result of interaction with a high-power Ar^+ laser beam. Our experiments show that the thermal effect of the interaction makes the glass matrix, with a thin layer of silver ions, behave as an uniaxial optical medium, with axis along the direction of beam propagation. The average index of refraction of the interaction area was measured, and it is shown that the index is increased. Our experimental results show that the induced anisotropy restricts the application of the microlenses, which are made by the interaction of pulsed laser beams with the ion-exchanged glasses [22, 23], for the polarized white light.

Acknowledgments Authors are grateful to Prof. M.T. Tavassoly from University of Tehran, for valuable discussions. We also appreciate assistance of Mr. J. Mostafavi-Amjad in sample preparation, from Institute for Advanced Studies in Basic Sciences (IASBS). Some parts of Experiments are done in IASBS. A. Nahal thanks International Center for Theoretical Physics (ICTP, Italy) for its support. We also are grateful to Dr. M. Nouri from University of Tehran for correcting the English language of this paper.

Appendix A

According to the Fig. 6a the phase difference equals to:

$$\delta = \frac{2\pi}{\lambda''}AB'' + \frac{2\pi}{\lambda}B''C - \frac{2\pi}{\lambda'}AB' \qquad \text{(a)}$$

with $AB'' = \frac{d}{\cos\theta''}$, $AB' = \frac{d}{\cos\theta'}$, $B''C = d\sin\theta_1$ $(\tan\theta' - \tan\theta')$ and using the Snell's law with $n_1 = 1$ for air, we have:

$$\delta = \frac{2\pi d}{\lambda}(n''\cos\theta'' - n'\cos\theta') \qquad \text{(b)}$$

If we take the AB' beam as the ordinary beam, then:

$$n' := n_o, \quad \theta' := \theta_o$$

$$\sin\theta_1 = n_o\sin\theta_o \quad \Rightarrow \quad n'\cos\theta' = n_o\sqrt{1 - \left(\frac{\sin\theta_1}{n_o}\right)^2} \qquad \text{(c)}$$

For the extraordinary beam we can write:

$$\theta'' := \theta_e \Rightarrow n''\sin\theta_e = \sin\theta_1 \qquad \text{(d)}$$

If the optical axis is normal to the surface, then the relation between n' and n_e can be obtained from the Fresnel's formula:

$$n'' = \frac{n_o n_e}{\sqrt{n_o^2\sin^2\theta_e + n_e^2\cos^2\theta_e}} \qquad \text{(e)}$$

Therefore, using Eqs. d, e and Fig. 6a we obtain:

$$\cot^2\theta_e = \frac{n_o^2 n_e^2 - n_o^2 \sin^2\theta_1}{n_e^2 \sin^2\theta_1} \quad \text{(f)}$$

After some simple trigonometric calculation and using Eqs. d, e, and f the relation for $n''\cos\theta''$ could be written as:

$$n''\cos\theta'' = \frac{n_o}{n_e}\sqrt{n_e^2 - \sin^2\theta_1} \quad \text{(g)}$$

Substituting Eqs. c and g in b we end up with:

$$\delta = \frac{2\pi d}{\lambda}\left(\frac{n_o}{n_e}\sqrt{n_e^2 - \sin^2\theta_1} - n_o\sqrt{1 - \left(\frac{\sin\theta_1}{n_o}\right)^2}\right) \quad \text{(h)}$$

References

1. Born M, Wolf E (1964) Principle of optics. Pergamon, Oxford
2. Chen X, Berger H (1999) J Phys: Condens Matter 11:7377
3. Froehly L, Verrier I, Froehly C, Burn G, Veillas C (1999) Opt Commun 167:27
4. Petrov DV, Gomes ASL, De Araujo CB (1994) Phys Rev B 50:9092
5. Chen X, Gonzalez S (1998) Appl Phys B 67:611
6. Foster JD, Osternik LM (1970) J Appl Phys 41(9):3656
7. Sims SD, Stein A, Roth C (1967) Appl Opt 6(3):579
8. Eichler HJ, Haase A, Menzel R, Siemoneit A (1993) J Phys D: Appl Phys 26:1884
9. Ayras PH, Friberg AT, Kaivola MAJ, Salomaa MM (1999) Appl Opt 38(25):5399
10. Chen X, Chaux R (1999) Opt Commun 171:119
11. Sims SD, Stein A, Roth C (1966) Appl Opt 5(4):621
12. Chen X, Calemczuk R, Salce B, Lavorel B, Akir C, Rajanoha L (1999) Solid State Commun 110:431
13. Chen X, Lavorel B, Dreier T, Genetier N, Misserey H, Michaut X (1998) Opt Commun 153:301
14. Koechner W, Rice DK (1970) IEEE J Quant Electron QE-6(9):557
15. Tikhomirov VK, Elliott SR (1994) Phys Rev B 49:17476
16. Kolobov AV, Lyubin VM, Tikhomirov VK (1992) Philos Mag Lett 65:67
17. Nahal A, Khalesifard HRM, Mostafavi-Amjad J (2004) Appl Phys B 79:513
18. Nahal A, Miloslavsky VK, Ageev LA (1998) Opt Commun 154:234
19. Chen X, Lavorel B, Boquillon JP, Saint-Loup R, Jannin M (1998) Solid-State Electron 42:1765
20. Nahal A, Mostafavi-Amjad J, Ghods A, Khajehpour MRH, Reihani SNS, Kolahchi MR (2006) J Appl Phys 100:053503
21. Nahal A, Khalesifard HRM (2007) Opt Mater 29:987
22. Kaganovski Yu, Antonov I, Bass F, Rosenbluh M (2001) J Appl Phys 89:8273
23. Antonov I, Bass F, Kaganovski Yu, Rosenbluh M (2003) J Appl Phys 93:2343
24. http://www.aqua.epfl.ch./projects.html
25. http://www.electronicimaging.org/program/04/
26. Najafi SI (1992) Introduction to glass integrated optics. Artech House, Boston
27. Nahal A, Rezae N (2005) In: Proc. 12th Conf. on Optics and Photonics, Shiraz Univ., Iran, pp 537–539 (In Persian)
28. Kreibig U, Vollmer M (1995) Optical properties of metal clusters. Springer, Berlin
29. Horowitz M, Daisy R, Werner O, Fischer B (1992) Opt Lett 17(7):475
30. Durbin SD, Arakelian SM, Shen YR (1981) Opt Lett 6(9):411
31. http://www.tulane.edu/~sanelson/geo1211/interference_of_light.htm
32. Pedrotti FL, Pedrotti LS (1993) Introduction to optics. Prentice Hall, New Jersey
33. Takeda S, Yamamoto K, Matsumoto K (2000) Non-Crystalline Solids 265:133
34. Martin M, Videau JJ, Canioni L, Adamietz F, Sarger L, Le Flem G (2000) Appl Opt 39:435